Control of Electrical Conductivity by Supramolecular Charge-Transfer Interactions in (Dithiolene)metalate–Viologen Ion Pairs

I. Nunn, B. Eisen, R. Benedix,† and H. Kisch*

Institut für Anorganische Chemie der Universität Erlangen-Nürnberg, D-91058 Erlangen, Germany

Received February 25, 1994[⊗]

Ion-pair charge-transfer (IPCT) complexes $\{A^{2+}[ML_2]^{2-}\}$, M = Ni, Pd, Pt, and Cu, between bipyridinium acceptors and (dithiolene)metalate donors exhibit in the solid state IPCT bands the energy of which increases linearly according to the Hush relation with more positive driving force (ΔG_{12}) of electron transfer from $[ML_2]^{2-}$ to A^{2+}. The electronic interaction between the two redox states is in the typical range of outer-sphere complexes as indicated by the values for the electronic-exchange integral of about 300 and 360 cm^{-1} for the nickel, platinum, and palladium compounds, respectively. The total reorganization energy of 32 complexes is 80 kJ/mol and exceeds the previously reported solution value by about 20 kJ/mol. According to the dependence of the specific electrical conductivity σ of pressed powder pellets on ΔG_{12} the compounds are divided into two classes. When both donor and acceptor can acquire a planar geometry (class I) it is found that log σ linearly increases from 10^{-11} to 10^{-3} Ω^{-1} cm $^{-1}$ upon varying ΔG_{12} from 0.7 to −0.1 eV. Similarly, log σ increases also linearly with decreasing free activation energy (ΔG^*) of electron transfer as calculated from the Hush–Marcus model. Contrary to that, neither the driving force nor ΔG^* has a significant influence on the conductivity when one of the ion pair components is nonplanar (class II). A hitherto unknown weak absorption band of the $[M(dmit)_2]^{2-}$component, $dmit^{2-}$ = 2-thioxo-1,3-dithiol-4,5-dithioalte, is detected at 1200–1500 nm and assigned to a ligand-centred transition on the basis of an MO calculation.

Introduction

The control of electrical conductivity of charge-transfer (CT) complexes by adjusting the redox properties of the components has been investigated in detail for organic systems. These were usually obtained from neutral components,[1,2] and classical examples are combinations of tetracyanoquinodimethane (TCNQ) acceptors with tetrathiafulvalene (TTF) or another donor. When the latter is 2,3,6,7-tetramethoxy-9,10-diselenaanthracene, the specific electrical conductivity (σ) increases from 10^{-10} to 10^{-6} $\Omega^{-1}cm^{-1}$ when the driving force of electron transfer from the donor to the acceptor ΔG_{12}, which is adjustable by variation of the acceptor redox potential, is increased from 0.7 to 0.17 eV.[3,4] Contrary to that, σ is lowered from 10 to 10^{-6} Ω^{-1} cm^{-1} when TTF is employed as donor, in which case ΔG_{12} varies from +0.23 to −0.35 eV.[3,4] The reason for this opposite behavior may be that rather structural than CT effects are dominating.[3,4]

In contrast to organic CT complexes, only a few inorganic systems have been investigated in this direction.[5–7] Initial evidence for a positive CT effect of the redox active organic cation methylene blue (MB^+) on the conductivity of $[Ni(mnt)_2]^{2-}$ salts[8,9] could not be reproduced later.[10] Accordingly, no CT band was detectable for $(MB^+)_2[M(mnt)_2]$, mnt^{2-} = maleonitrile-1,2-dithiolate, M = Ni, Pd, Pt, and Cu, respectively.[10] Similarly, no obvious relation between redox properties of the dianions (M = Ni, Pd, Pt) was observed when MB^+ was replaced by an inorganic redox active cation like Cu^{2+}.[11,12] In addition, polarization effects ("heavy atom effects") of the metal may be important as was suggested to be partly responsible for the increase of σ from 10^{-5} to 10^{-3} Ω^{-1} cm^{-1} when palladium in $(TTF)_2[M(mnt)_2]$ is replaced by platinum.[4]

The electrical properties of neutral metal dithiolenes were first measured by Schrauzer and Rosa.[13] Later the mono- and dianionic complexes were investigated by Underhill[14] and Rosseinsky[8,9] in order to study the influence of counterions. Recently, compounds with non-integral oxidation states, especially of those containing the $dmit^{2-}$ ligand were intensively investigated since they may become superconductors at very low temperature and very high pressure.[15] Polymeric metal dithiolenes[16] may reach conductivities up to 30 $\Omega^{-1}cm^{-1}$.

Recently we have prepared ion pair charge-transfer (IPCT) complexes of the type $\{A^{2+}[ML_2]^{2-}\}$ wherein the acceptor A^{2+} is a dicationic 4,4′- or 2,2′-bipyridinium derivative and $[ML_2]^{2-}$ is a planar metal dithiolene (Figure 1). Throughout this paper donor and acceptor charges are usually omitted and formulas are written as $A[ML_2]$.

It was shown that the solid state structure of the prototype complex $MV[Ni(mnt)_2]$ consists of mixed donor–acceptor columns (DADA) with an approximately cofacial arrangement

† Present address: Hochschule für Technik, Wirtschaft und Kultur Leipzig (FH), D-04251 Leipzig, Germany.

⊗ Abstract published in *Advance ACS Abstracts,* September 15, 1994.

(1) Foster, R. *Molecular Association*; Academic Press: London, 1979.
(2) Torrance, J. B. *Mol. Cryst. Liq. Cryst.* **1985**, *126*, 55.
(3) Wheland, R. C.; Gillson, J. L. *J. Am. Chem. Soc.* **1976**, *98*, 3916.
(4) Wheland, R. C. *J. Am. Chem. Soc.* **1976**, *98*, 3926.
(5) Keller, H. J.; Soos, G. Z. *Top. Curr. Chem.* **1985**, *127*, 169.
(6) Alcacer, L.; Novais, H.; *Linear Chain 1,2-Dithiolene Complexes.* In *Extended Linear Chain Compounds;* Miller, J. S., Ed.; Plenum Press: New York, London, 1983; Vol 3, p 319.
(7) Alcacer, L. J.; Novais, H. M.; Pedroso, F. P.; Flandrois, S.; Coulon, C.; Chasseau, D.; Gaultier, *J. Solid State Commun.* **1980**, *35*, 945.
(8) Rosseinsky, D. R.; Malpas, R. E. *J. Chem. Commun.* **1977**, 455.
(9) Rosseinsky, D. R.; Malpas, R. E. *J. Chem. Soc., Dalton Trans.* **1979**, 749.
(10) Tonge, J. S.; Underhill, A. E. *J. Chem. Soc., Dalton Trans.* **1984**, 2333.
(11) Underhill, A. E.; Ahmad, M .M.; Turner, D. J.; Clemenson, P. I.; Corneiro, K.; YueQiuan, S.; Mortensen, K. *Mol. Cryst. Liq. Cryst.* **1985**, *120*, 369.
(12) Manecke, G.; Wöhrle, D. *Makromolekulare Chem.* **1968**, *116*, 36.
(13) Rosa, E. J.; Schrauzer, G. N. *J. Phys. Chem.* **1969**, *73*, 3132.
(14) Clemenson, P. I. *Coord. Chem. Rev.* **1990**, *106*, 171.
(15) Cassoux, P.; Valade, L.; Kobayashi, H.; Clark, R. A.; Underhill, A. E. *Coord. Chem. Rev.* **1991**, *110*, 115.
(16) Rivera, N. M.; Engler, E.; Schumaker, R. R. *J. Chem. Soc., Chem. Commun.* **1979**, 184.

0020-1669/94/1333-5079$04.50/0

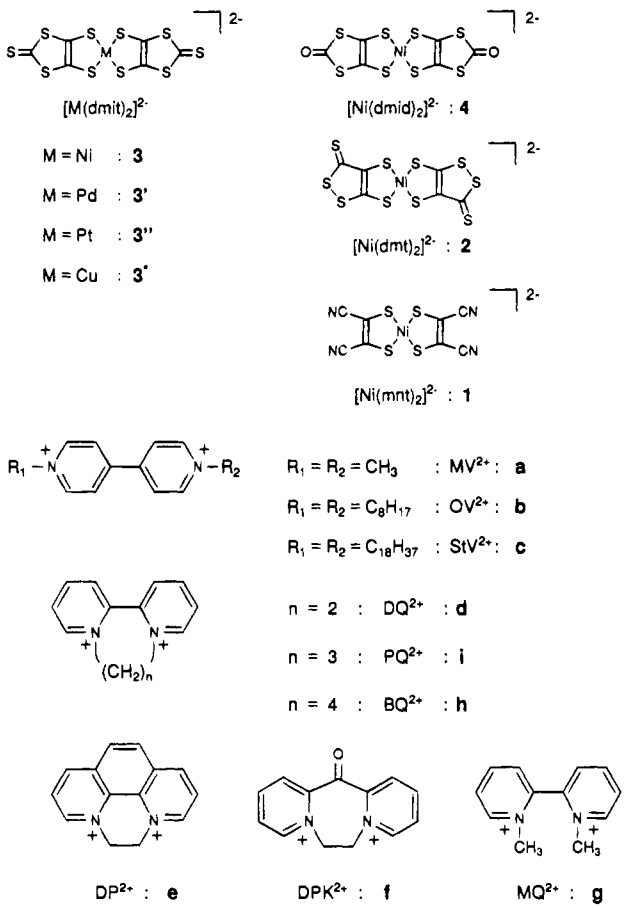

Figure 1.

of the two planar components.[17] From the spectroscopic properties of the solution IPCT band the parameter α^2, which describes the amount of charge transferred from $[ML_2]^{2-}$ to A^{2+} in the ground state contact ion pair, was calculated according to the Hush model[18,19] as 10^{-4}.[20] This means that the resulting decrease of Coulombic energy is so small that the solid state structure of a sequence of similar ion pairs should be dominated by electrostatic factors as long as the geometry of the components stays approximately the same. Therefore, these IPCT complexes should be better candidates to study the effect of varying CT interaction on the electrical conductivity than the few systems mentioned above. We therefore first have synthesized a number of d^8-metal IPCT complexes which all have approximately planar components. Besides Ni also Pd and Pt were introduced to test for mutual polarization effects. Second, the influence of increasingly nonplanar acceptors was studied. Third, it was investigated whether similar effects may occur when a d^9 metal like Cu(II) is involved. Part of this work has been communicated in short form.[21,22]

Experimental Section

Materials, Methods, and Preparations. $MVCl_2 \cdot 3H_2O$ was purchased from Fluka and used without further purification. The compounds $OVBr_2$,[23] $StVBr_2$,[24] $MQ(BF_4)_2$,[25] $BQBr_2$,[26] $PQBr_2$,[26] $DQBr_2$,[26] $DPBr_2$,[27] DPKBr$_2$,[28] EPSPBr,[24] $(NBu_4)_2[Ni(dmit)_2]$,[29] $(NBu_4)_2[Pd(dmit)_2]$,[29] $(NBu_4)_2[Pt(dmit)_2]$,[29] $(NBu_4)_2[Cu(dmit)_2]$,[29] $(NBu_4)_2[Ni(dmid)_2]$,[30] $(NBu_4)_2[Ni(dmt)_2]$,[31] $(NBu_4)_2[Ni(mnt)_2]$,[32] $OV[Ni(dmit)_2]$,[24] $StV[Ni(dmit)_2]$,[24] $DQ[Ni(dmit)_2]$,[24] $OV[Pt(dmit)_2]$,[33] $DQ[Pt(dmit)_2]$,[33] $OV[Ni(dmt)_2]$,[33] $DQ[Ni(dmt)_2]$,[33] $DQ[Ni(mnt)_2]$,[24] $MQ[Ni(dmit)_2]$,[20] $PQ[Ni(dmit)_2]$,[20] $BQ[Ni(dmit)_2]$,[20] $MQ[Pt(dmit)_2]$,[20] $PQ[Pt(dmit)_2]$,[20] $BQ[Pt(dmit)_2]$,[20] $MQ[Cu(dmit)_2]$,[20] $PQ[Cu(dmit)_2]$,[20] and $BQ[Cu(dmit)_2]$,[20] were prepared according to literature methods. Syntheses of the new compounds were performed under inert atmosphere (nitrogen or argon) using standard Schlenk techniques. Reagent grade solvents were dried by conventional methods and distilled under nitrogen prior to use. The ion-pair complexes were obtained in yields of 45−99% by the general procedure as described below.

Synthesis of MV[Ni(dmit)$_2$](3a). A solution of 0.19 g (0.62 mmol) of $MVCl_2 \cdot 3H_2O$ in 60 mL of acetone/water (2:1) was added dropwise to 0.58 g (0.62 mmol) of $(NBu_4)_2[Ni(dmit)_2]$ dissolved in 150 mL of acetone. Rapidly a dark grayish blue precipitate was formed which was collected by filtration after 24 h. The microcrystalline solid carefully washed with methanol was dried in high vacuum. Yield: 320 mg (81%).

The palladium and platinum homologues were synthesized analogously by using the PF_6^- salt of the acceptor component dissolved in acetone. The PF_6^- salts were prepared by metathesis of the corresponding dihalogenides with NH_4PF_6 in aqueous solution.

Physical Measurements. Microanalyses were performed on a Carlo Erba Model 1106 elemental analyzer. Infrared spectra (KBr pellet) were recorded on a Perkin-Elmer Model 983 instrument. Diffuse reflectance spectra were measured relative to corundum (Hoechst Ceram Tec) with a Shimadzu Model 3101 spectrophotometer equipped with an integrating shere unit. The onset of the IPCT band (E_{IPCT}) was determined according to the method by Karvaly and Hevesi, originally developed for inorganic semiconductors,[34] which is independent on the sample concentration. Within the linear decrease of absorption on the low-energy side of the IPCT band 5−6 points are selected and the term $\{[F(R_\infty)h\nu]^2\}$, $F(R_\infty) = (1 - R_\infty)^2/2R_\infty$ (Kubelka−Munk function), is calculated for each of them. A plot of the first term vs $h\nu$ affords a straight line which intersects the abscissa at the value of E_{IPCT}.

Cyclic voltammetric experiments were carried out on an EG&G Princeton Applied Research Model PAR 264A potentiostat by using a conventional three-electrode assembly consisting of a glassy-carbon working electrode, a platinum wire as counter electrode, and a Ag/AgCl reference electrode in saturated KCl solution. All measurements were performed in dry and nitrogen-degassed acetonitrile solutions containing 10^{-3} M substrate, 0.1 M NBu_4PF_6 as supporting electrolyte, and ferrocene as internal reference. Potentials were calibrated relative to the ferrocene/ferrocenium redox couple and referenced vs SCE by $E_{1/2}(Fc^{+/0}) = 0.39$ V.

Specific resistivities were measured for compacted pellets at ambient conditions by the conventional two-probe method as described previously.[24] Differences in applied pressure have only a minor influence as indicated by the values of log σ of −6.02, −5.92, and −5.98 for $MV[Ni(dmit)_2]$ at 5.8, 3.8, and 2.9 kbar, respectively. Partial oxidation by air seems to be unimportant as shown by the values of log σ of −4.82 and −4.91 for $OV[Ni(dmit)_2]$ at 2 h and 3 days after pellet preparation, respectively. Activation energies E_a were determined by measuring conductivities in the range of 20−120 °C. For that purpose

(17) Kisch, H.; Fernandez, A.; Wakatsuki, Y.; Yamazaki, H. Z. *Naturforsch.* **1985**, *40b*, 292.
(18) Hush, N. S. *Progr. Inorg. Chem.* **1967**, *8*, 391.
(19) Marcus, R. A.; Sutin, N. *Comments Inorg. Chem.* **1986**, *5*, 119.
(20) Dümler, W.; Kisch, H. *New. J. Chem.* **1991**, *15*, 649.
(21) Kisch, H.; Nüsslein, F.; Zenn, I. Z. *Anorg. Allg. Chem.* **1991**, *600*, 67.
(22) Kisch, H.; Dümler, W.; Nüsslein, F.; Zenn I.; Chiorboli, C.; Scandola, F.; Albrecht, W.; Meier, H. Z. *Phys. Chem.* **1991**, *170*, 117.
(23) Maidan, R.; Goren, Z.; Becker, J. Y.; Willner, I. *J. Am. Chem. Soc.* **1984**, *106*, 6217.
(24) Nüsslein, F.; Peter, R.; Kisch, H. *Chem. Ber.* **1989**, *122*, 1023.
(25) Hünig, S.; Gross, J.; Schenk, W. *Liebigs Ann. Chem.* **1973**, 324.
(26) Homer, R. F.; Tomlinson, T. E. *J. Chem. Soc.* **1960**, 2498.
(27) Hünig, S.; Gross, J.; Lier, E. F.; Quast, H. *Liebigs Ann. Chem.* **1973**, 339.
(28) Black, A. L.; Summers, L. A. *J. Chem. Soc. C* **1970**, 2394.
(29) Steimecke, G.; Sieler, H. J.; Kirmse, R.; Hoyer, E. *Phosphorus Sulfur* **1979**, *7*, 49.
(30) Olk, R. M.; Dietzsch, W.; Köhler, K.; Kirmse, R.; Reinhold, J.; Hoyer, E.; Golic, L.; Olk, B. Z. *Anorg. Allg. Chem.* **1988**, *567*, 131.
(31) Steimecke, G.; Sieler, H. J.; Kirmse, R.; Dietzsch, W.; Hoyer, E. *Phosphorus Sulfur*, **1982**, *12*, 237.
(32) Billig, E.; Williams, R.; Bernal, I.; Waters, J. H.; Gray, H. B. *Inorg. Chem.* **1964**, *3*, 663.
(33) Nüsslein, F. *Doctoral Thesis*, Erlangen-Nürnberg, 1989.
(34) Karvaly, B.; Hevesi, I. Z. *Naturforsch.* **1971**, *26a*, 245.

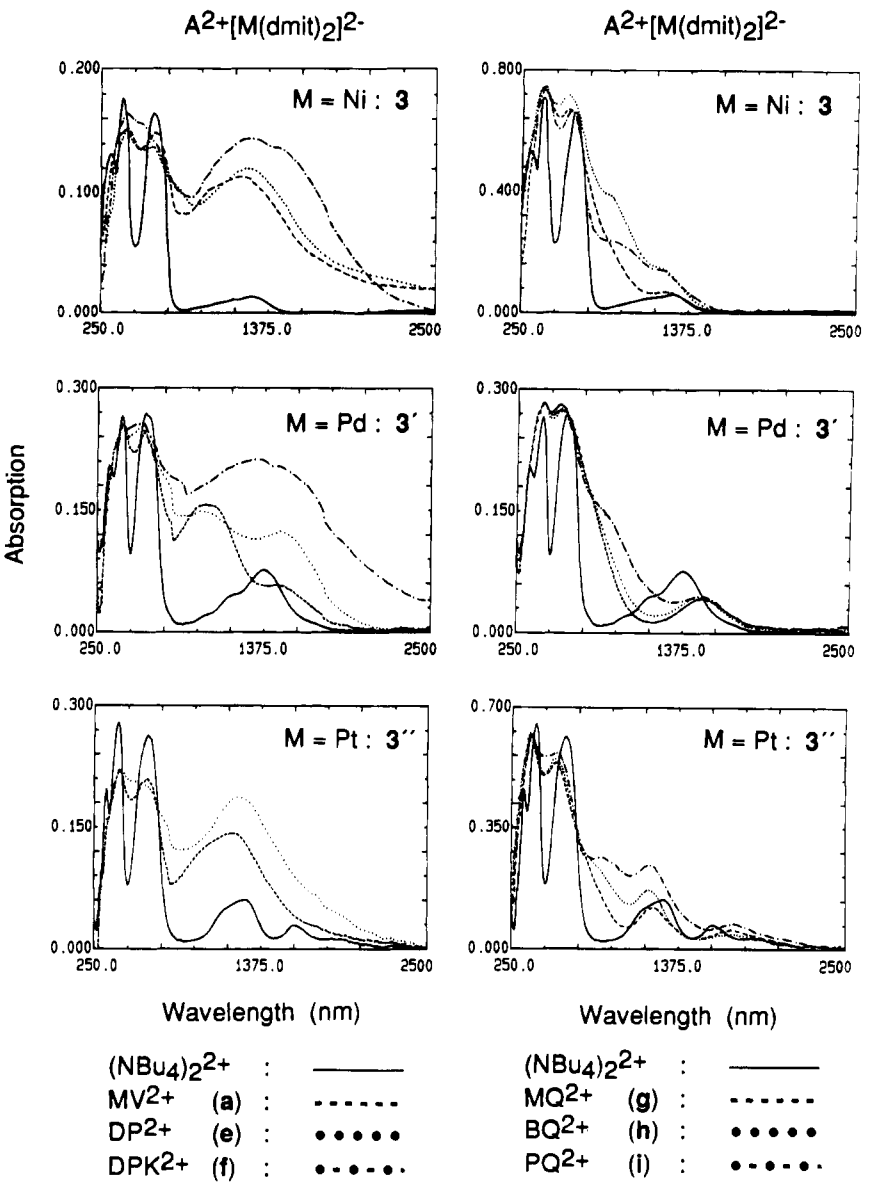

Figure 2. Diffuse reflectance spectra of A[M(dmit)$_2$] as compared to (NBu$_4$)$_2$[M(dmit)$_2$], M = Ni, Pd, and Pt.

the contacted pellet was adjusted in a Teflon cell containing brass contacts and a Ni/Cr−Ni thermoelement. The cell was immersed into an oil bath and resistivity was measured during the heating period. Activation energies do not depend on the nature of the electrical contact between electrode and sample since both the contacted and the noncontacted pellet have the same value of 0.35 eV as obtained for DP[Ni(dmit)$_2$].

For the calculation of α^2 for MV[M(dmit)$_2$] according to eq 1 the following values were used: $\epsilon_{max} = 100$ M^{-1} cm^{-1}; $d = 3.4 \times 10^{-8}$ cm;[35] $\Delta\tilde{\nu}_{1/2} = 3500$, 4200, and 3200 cm^{-1} for M = Ni, Pd, and Pt, respectively; $E_{IPCT} = 6900$, 8400, and 7300 cm^{-1} in the same sequence, respectively. The extended Hückel method has been used in its standard version, with charge iteration on the central atom.[36,37] In the calculation the so-called "weighted H_{ij} formula" for the diagonal elements was used in order to take into account the phenomenon of counter-intuitive orbital mixing common in calculations of transition-metal complexes.[38] Single Slater-type orbitals were used for the main group elements and the s- and p-functions of the metal, while the d-wave functions were taken as a contracted linear combination of the two Slater-type functions published by Alvarez et al.[39]

$$\alpha^2 = 4.24 \times 10^{-20} \epsilon_{max} \Delta\tilde{\nu}_{1/2} / d^2 E_{IPCT} \quad (1)$$

Results

The new compounds are obtained as amorphous powders by addition of the bipyridinium salt to a solution of the corresponding tetrabutylammonium (dithiolene)metalate in acetone. Attempts to obtain single crystals for X-ray analysis failed, but from the comparison of IR and diffuse reflectance spectra with those of MV[Ni(mnt)$_2$], the structure of which is known,[17] one can assume a similar donor−acceptor arrangement. In order to change ΔG_{12}, the reduction potentials of donor and acceptor were varied in the range from +0.22 to −0.29 and −0.75 to −0.06 V, respectively. As an example, values of +0.22, +0.06, −0.14, and −0.29 V are obtained when in [NiL$_2$]$^{2-}$ the mnt^{2-} ligand is substituted by dmt^{2-}, dmit^{2-}, and dmid^{2-}, respectively (Figure 1). While the slightly twisted or planar 4,4'- and 2,2'-bipyridinium acceptors MV^{2+} (**a**), OV^{2+} (**b**), StV^{2+} (**c**) DQ^{2+} (**d**), DP^{2+} (**e**), and DPK^{2+} (**f**) have potentials of −0.43, −0.42, −0.46, −0.36, −0.32, and −0.06, respectively, the values of

(35) Schmauch, G.; Knoch, F.; Kisch, H. *Chem. Ber.*, in press.
(36) Hoffmann, R. *J. Chem. Phys.* **1963**, *39*, 1397.
(37) Ballhausen, C. J.; Gray, H. B. *Molecular Orbital Theory*; W. A. Benjamin: New York, Amsterdam, 1965.
(38) Ammeter, J. H.; Bürgi, H. B.; Thibeault, J. C.; Hoffman, R. *J. Am. Chem. Soc.* **1978**, *100*, 3686.
(39) Alvarez, S.; Vincente, R. Hoffman, R. *J. Am. Chem. Soc.* **1985**, *107*, 6253.

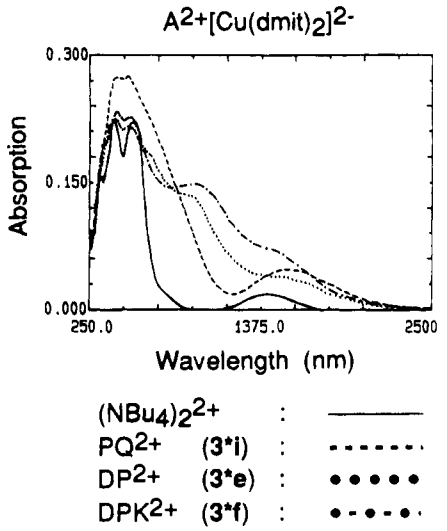

Figure 3. Diffuse reflectance spectra of A[Cu(dmit)$_2$] as compared to (NBu$_4$)$_2$[Cu(dmit)$_2$].

the strongly twisted 2,2′-derivatives MQ^{2+} (**g**), BQ^{2+} (**h**), and PQ^{2+} (**i**) are located in the more negative range of −0.75, −0.66, and −0.56 V.

In the IR spectra a mutual IPCT interaction should be indicated by changes in the out-of-plane aromatic C−H vibration γ(C−H) of the bipyridinium and in the ν(C=C) and ν(C−S) vibrations of the metal dithiolene component. This expectation arises from the fact that in DQBr$_2$ the γ(C−H) vibration decreases from 793 to 781 cm^{-1} when bromide is replaced by the better donor iodide[40] and ν(C−S) increases from 885 to 902 cm^{-1} while ν(C=C) decreases from 1440 to 1353 cm^{-1} when $[Ni(dmit)_2]^{2-}$ is oxidized to the monoanion.[29] However, in DQ-[NiL$_2$] γ(C−H) changes from 768 to 731, 756, and 755 cm^{-1} when L is varied in the direction of increasing reducing power from mnt^{2-} to dmt^{2-}, $dmit^{2-}$, and $dmid^{2-}$, respectively. Thus, although there is a general decrease, it does not correlate with the sequence of reduction potentials. Changes in the characteristic vibration frequencies of the dithiolene part, which occur upon variation of the acceptor, are small and have no obvious relation to the redox properties.

UV−vis-near-IR diffuse reflectance spectra are summarized in Figures 2−4. As compared to the corresponding tetrabutylammonium complexes, introduction of the bipyridinium cation induces appearance of new absorptions in the range of 500−1500 and around 400 nm. The location of the latter does not depend on the reduction potential of A^{2+}, while that of the former shifts to higher energy when the potential becomes more negative. As compared to the lowest-energy absorption of (NBu$_4$)$_2$[M(dmit)$_2$], M = Ni, Pd, and Pt, this new band appears at about the same or lower energy in the case of the better acceptors **a**−**f** (Figure 2), except for the two palladium compounds **3′a** and **3′e**, while it is located at higher energy in the case of the poorer acceptors **g**, **h**,and **i**. The latter applies also for all $[Cu(dmit)_2]^{2-}$ compounds (Figure 3), while the limited number of the dmt^{2-} and $dmid^{2-}$- complexes (Figure 4) does not allow a similar division.

Specific electrical conductivities (σ) were obtained by measuring the resistance of presssed powder pellets contacted on two sides by silver paint.[24] These two-probe measurements did not differ from the four-probe method as demonstrated by the values 4×10^{-3} and 3.6×10^{-3} Ω^{-1} cm^{-1}, respectively, found for NBu$_4$[Pd(dmit)$_2$].[41] The reproducibility of σ is ±5% when pressing and contactation from an unique sample is

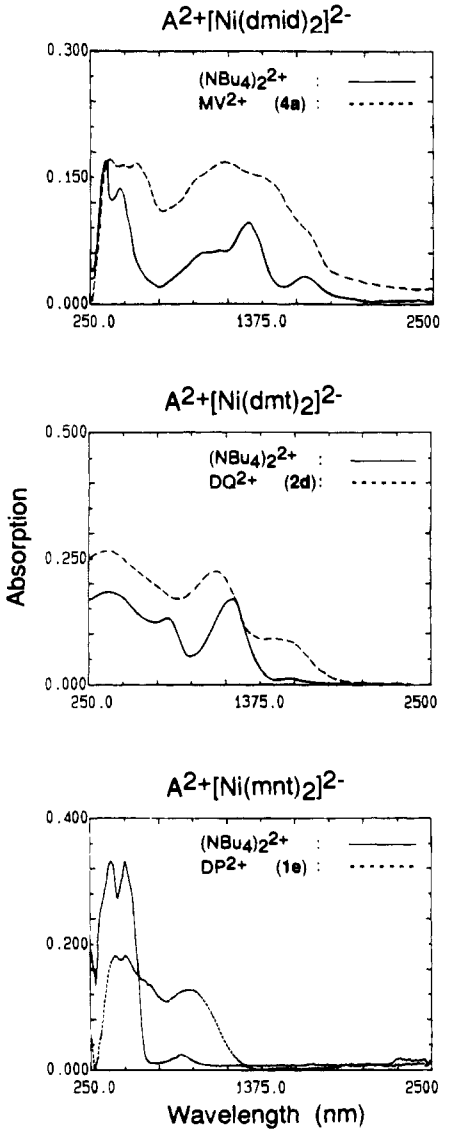

Figure 4. Diffuse reflectance spectra of A[NiL$_2$], L = $dmid^{2-}$, dmt^{2-}, and mnt^{2-}, as compared to (NBu$_4$)$_2$[NiL$_2$].

repeated, while it is ±50% when the sample is synthesized again. Influences of air or differing pressures are negligible. The conductivities of the 39 samples investigated span a range of 10^{-11} to 10^{-3} Ω^{-1} cm^{-1} and are summarized in Table 1.

Activation energies (E_a, Table 1) vary from 0.15 to 1.44 eV and were obtained by measuring σ in the range from 20 to 120 °C. At higher temperatures the silver paste starts to melt away. From the slope of a plot of log σ vs $1/T$ the value of E_a is obtained according to the relation $\log \sigma = \log \sigma_o - 0.434E_a/kT$. All plots exhibited excellent linearity.

Discussion

Electronic Spectra. Electronic absorption spectra of the (dithiolene)metalate part have been interpreted for $[M(mnt)_2]^{2-}$ complexes, M = Ni.[42] By analogy, the bands of the corresponding dmit complexes at about 610 nm (M = Ni, Pt), 570 nm (M = Pd), 415 nm (M = Ni), and 410 nm (M = Pd, Pt), respectively, are assignable to CTML ($3b_{3g} \rightarrow 3a_u$; Figure 5) and CTLM ($2a_u$, $3b_{1u} \rightarrow 8b_{1g}$) transitions, respectively. The lowest-energy bands in the near-IR range 1200−1500 nm have not been mentioned in the literature. From the low absorptivities

(40) Haque, R.; Lilley, S. *J. Agr. Food Chem.* **1972**, *20*, 57.
(41) Peter, R. *Diploma Thesis*, Erlangen-Nürnberg, 1986.
(42) Shupack, S. I.; Billig, E.; Clark, R. J. H.; Williams, R.; Gray, H. B.; *J. Am. Chem. Soc.* **1964**, *86*, 4594.

Table 1. Reduction Potentials of Solvent−Separated Ions, Free Reaction (ΔG_{12}) and Activation (ΔG^*) Enthalpies of Electron Transfer between the Ions, and Electrical Parameters (log σ, E_a) and Onset of IPCT Band (E_{IPCT}) of Solid Ion Pairs

compd	no.	$E(D^{-/2-})^a$	$E(A^{2+/+})^a$	$\Delta G_{12}{}^b$	log σ^c	$E_a{}^b$	$\Delta G^{*\,b}$	$E_{IPCT}{}^b$
MQ[Ni(dmit)$_2$]	**3g**	−0.14	−0.75	+0.61	−5.57	0.33	0.62	1.36
MQ[Pd(dmit)$_2$]	**3′g**	−0.02	−0.75	+0.73	−6.32	0.29	0.75	1.51
MQ[Pt(dmit)$_2$]	**3″g**	−0.16	−0.75	+0.59	−4.60		0.59	1.29
BQ[Ni(dmit)$_2$]	**3h**	−0.14	−0.66	+0.52	−6.15	0.42	0.54	1.27
BQ[Pd(dmit)$_2$]	**3′h**	−0.02	−0.66	+0.64	−6.39	0.26	0.66	1.40
BQ[Pt(dmit)$_2$]	**3″h**	−0.16	−0.66	+0.50	−4.04		0.52	1.24
PQ[Ni(dmit)$_2$]	**3i**	−0.14	−0.56	+0.42	−5.39	0.35	0.45	1.12
PQ[Pd(dmit)$_2$]	**3′i**	−0.02	−0.56	+0.54	−6.26	0.28	0.55	1.22
PQ[Pt(dmit)$_2$]	**3″i**	−0.16	−0.56	+0.40	−3.89		0.43	1.11
StV[Ni(dmit)$_2$]	**3c**	−0.14	−0.46	+0.32	−6.60		0.35	0.92
StV[Pd(dmit)$_2$]	**3′c**	−0.02	−0.46	+0.44	−10.09	0.75	0.46	1.08
StV[Pg(dmit)$_2$]	**3″c**	−0.16	−0.46	+0.30	−7.59	0.45	0.32	0.83
MV[Ni(dmit)$_2$]	**3a**	−0.14	−0.43	+0.29	−5.92	0.26	0.32	0.86
MV[Pd(dmit)$_2$]	**3′a**	−0.02	−0.43	+0.41	−6.96	0.39	0.43	1.04
MV[Pt(dmit)$_2$]	**3″a**	−0.16	−0.43	+0.27	−5.60	0.31	0.32	0.91
OV[Ni(dmit)$_2$]	**3b**	−0.14	−0.42	+0.28	−6.85	0.54	0.32	0.89
OV[Pd(dmit)$_2$]	**3′b**	−0.02	−0.42	+0.40	−9.00	0.59	0.43	1.07
OV[Pt(dmit)$_2$]	**3″b**	−0.16	−0.42	+0.26	−7.54	0.51	0.32	0.93
DQ[Ni(dmit)$_2$]	**3d**	−0.14	−0.36	+0.22	−6.02	0.46	0.29	0.86
DQ[Pd(dmit)$_2$]	**3′d**	−0.02	−0.36	+0.34	−6.42	0.32	0.38	1.03
DQ[Pt(dmit)$_2$]	**3″d**	−0.16	−0.36	+0.20	−5.72	0.27	0.29	0.89
DP[Ni(dmit)$_2$]	**3e**	−0.14	−0.32	+0.18	−5.37	0.34	0.27	0.85
DP[Pd(dmit)$_2$]	**3′e**	−0.02	−0.32	+0.30	−5.80	0.27	0.36	1.00
DP[Pt(dmit)$_2$]	**3″e**	−0.16	−0.32	+0.16	−4.77	0.25	0.26	0.86
DPK[Ni(dmit)$_2$]	**3f**	−0.14	−0.06	−0.08	−3.50	0.15	0.16	0.71
DPK[Pd(dmit)$_2$]	**3′f**	−0.02	−0.06	+0.04	−5.40	0.17	0.21	0.81
StV[Ni(dmid)$_2$]	**4c**	−0.29	−0.46	+0.17	−7.81		0.25	0.77
MV[Ni(dmid)$_2$]	**4a**	−0.29	−0.43	+0.14	−5.55	0.34	0.24	0.77
OV[Ni(dmid)$_2$]	**4b**	−0.29	−0.42	+0.13	−4.80	0.31	0.24	0.81
DQ[Ni(dmid)$_2$]	**4d**	−0.29	−0.36	+0.07	−5.98	0.24	0.23	0.85
DQ[Ni(mnt)$_2$]	**1d**	+0.22	−0.36	+0.58	−10.90		0.58	1.20
DP[Ni(mnt)$_2$]	**1e**	+0.22	−0.32	+0.54	−8.28	0.57	0.54	1.18
OV[Ni(dmt)$_2$]	**2b**	+0.06	−0.42	+0.48	−8.34		0.49	1.09
DQ[Ni(dmt)$_2$]	**2d**	+0.06	−0.36	−0.42	−7.64	0.35	0.45	1.15
MQ[Cu(dmit)$_2$]	**3*g**	−0.02	−0.75	+0.73	<−11.00		0.73	1.35
BQ[Cu(dmit)$_2$]	**3*h**	−0.02	−0.66	+0.64	−7.52		0.64	1.35
PQ[Cu(dmit)$_2$]	**3*i**	−0.02	−0.56	+0.54	−8.19		0.55	1.28
DP[Cu(dmit)$_2$]	**3*e**	−0.02	−0.32	+0.30	−8.53	1.44	0.30	0.67
DPK[Cu(dmit)$_2$]	**3*f**	−0.02	−0.06	+0.04	−7.97	1.29	0.19	0.73

^{a} From cyclic voltammetry in MeCN, V vs SCE. ^{b} eV. ^{c} Ω^{-1} cm^{-1}.

(in solution 150, 210, and 350 M^{-1} cm^{-1} for Ni, Pd, and Pt at 1220, 1245, and 1210 nm, respectively) a metal-centered nature is suggested; however, there is not the expected blue-shift when Ni is replaced by the higher homologues. To clarify the origin of these bands, the MO diagram of $[Ni(dmit)_2]^{2-}$ was calculated by the EHT method (see Experimental Section) (Figure 5). As compared to the MO diagram of $[Ni(mnt)]^{2-}$,[42] two new allowed, x-polarized transitions, $4b_{1u} \rightarrow 6b_{2g}$ and $4b_{2g} \rightarrow 5b_{1u}$, emerge. Note that the orbitals involved have ligand character and are delocalized onto both dmit ligands. Thus the corresponding weak absorption bands at 1270 (shoulder at 1170 nm) and 1370 nm in the case of Ni, Pt, and Pd, respectively, may be characterized as $(\pi,\pi)^*$ or intraligand type. No assignment can be made for the weaker bands of the nickel and platinum complex at 1600 and 1950 nm (Figure 2).

Recently it was shown[20] that for a series of nickel and platinum mnt^{2-} and $dmit^{2-}$ complexes with the acceptors MQ^{2+}, BQ^{2+}, and PQ^{2+}, a plot of the maximum of the IPCT band in solution (E_{op}) against the driving force of electron transfer within the contact ion pair (ΔG_{IP}) follows the Hush relation[18] $E_{op} = \chi + \Delta G_{IP}$, wherein χ is the total reorganization energy. Due to the low absorptivity of the IPCT bands, ϵ-values are in the range 40−1000 M^{-1} cm^{-1} [20] and overlap with metal dithiolene bands, it is difficult to obtain E_{op} with sufficient accuracy from solution spectra. We therefore used the onset of the IPCT band, E_{IPCT}, which is accessible by a simple procedure from the diffuse reflectance spectra[34] (see Experimental Section) instead of E_{op}. Since the bands are very broad, the onset E_{IPCT} is red-shifted by about 100−200 nm from E_{op} values measured in solution. The free enthalpies of ion association[43] are irrelevant for the solid state, and ΔG_{IP} can be expressed as ΔG_{12} (eq 2), which

$$E_{IPCT} = \chi + \Delta G_{12} \quad (2)$$

$$A^{2+} + [ML_2]^{2-} \rightarrow A^{+} + [ML_2]^{-} \quad (3)$$

applies for the electron transfer between the free ions in solution (eq 3), and is easily obtained from the reduction potential difference of the two components. The corresponding values are summarized in Table 1, and a plot of E_{IPCT} versus ΔG_{12} for 32 complexes reveals the expected linear decrease of the energy of the IPCT transition with increasing exergonicity of the thermal electron transfer (Figure 6). Copper complexes were not included since the donor part may have a tetrahedral geometry as was reported for (1-ethylpyridinium)$_2$[Cu(dmit)$_2$].[44]

The slope of 0.9 deviates by 10% from the theoretical value of 1.0, which is not too surprising since it seems unlikely that the intrinsic barriers of electron transfer should be the same for all complexes. A slope of 1.39 has been reported from a plot of E_{op} obtained from solid state absorbance spectra for ion pairs consisting of the octahedral components $[Ru(NH_3)_6]^{3+}$ and $[Fe(CN)_5L]^{n-}$ (n = 3, 4; L = CO, CN^-, pyridine).[45] In solution similar ion pairs between $[Fe(CN)_6]^{4-}$ and $[Ru(NH_3)_5(pyridine)]^{3+}$

(43) Curtis, J. L.; Sullivan, B. P.; Meyer, T. J. *Inorg. Chem.* **1980**, *19*, 3833.
(44) Matsubayashi, G.; Takahashi, K.; Tanaka, T. *J. Chem. Soc., Dalton Trans.* **1988**, 967.
(45) Toma, H. E. *J. Chem. Soc., Dalton Trans.* **1980**, 471.

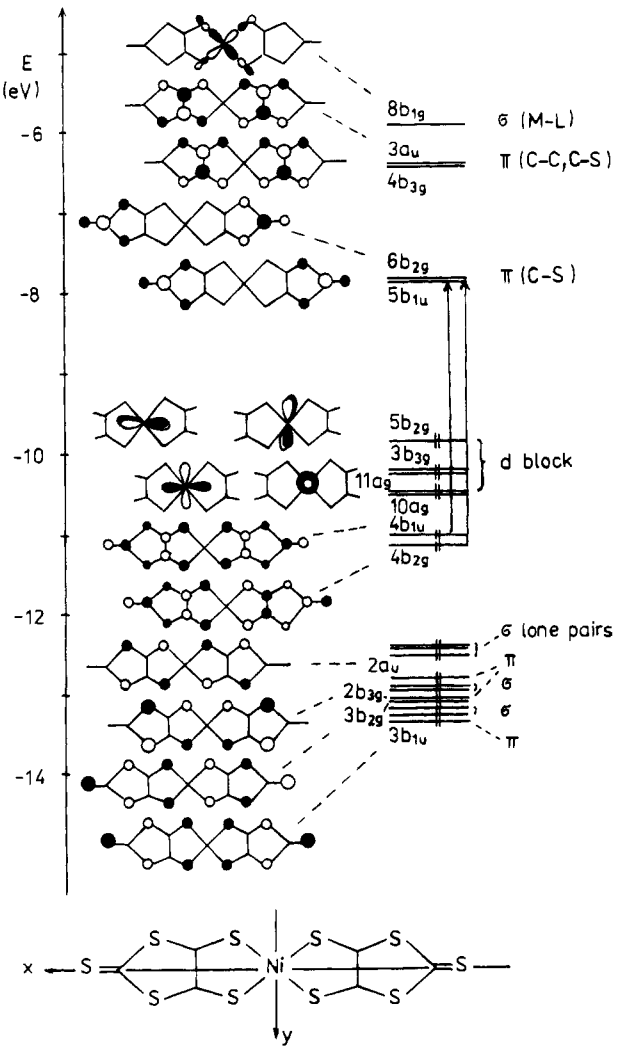

Figure 5. Basic features of the MO diagram of $[Ni(dmit)_2]^{2-}$.

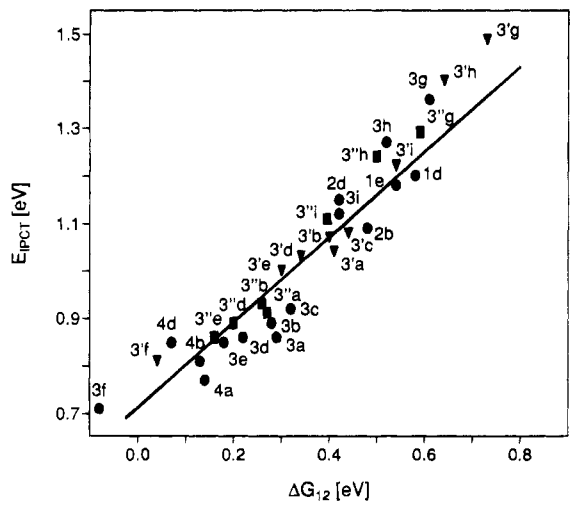

Figure 6. Plot of the onset energy of the IPCT band, obtained from diffuse reflectance spectra as function of ΔG_{12} as calculated from solution redox potentials: ●, Ni; ▼, Pd; ■, Pt.

afford a slope of 1.[46] From the intercept (Figure 6) a mean reorganization energy of 60 kJ/mol (0.63 eV) is calculated (Figure 6). To compare this with the solution value of about 50 kJ/mol obtained previously for the above mentioned $A[M(dmit)_2]$ complexes,[20] which are based on taking E_{op} as the energy at the maximum of the IPCT band, a mean value of about 20 kJ/mol has to be added since this is the average

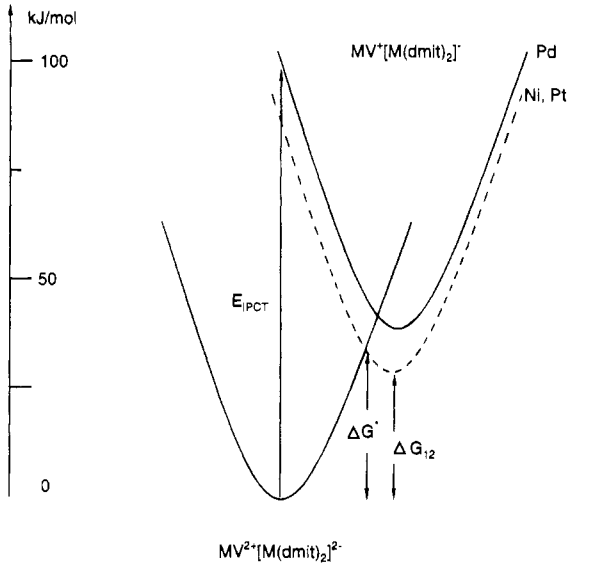

Figure 7. Relative positions of potential energy curves before and after electron transfer as obtained from the Hush–Marcus model.

amount by which the onset E_{IPCT} is red-shifted from the maximum in the diffuse reflectance spectra.

Within the Hush model the amount of charge transferred from the donor to the acceptor is given by the parameter α^2, which can be easily calculated from absorptivity, half-bandwidth, E_{IPCT} and the distance of the two components in the contact ion pair (See Experimental Section). The latter was taken from the X-ray analysis results of the corresponding mnt complexes since no data are available for the dmit compounds. Values of α^2 are in the range of 10^{-3}, which are typical for outer-sphere complexes.[47,48] The electronic coupling between the two redox states is weak as indicated by the values of 299, 360, and 295 cm^{-1} for the electron-exchange matrix element H_{DA} (equal to αE_{IPCT})[18] in the case of $MV[M(dmit)_2]$, M = Ni, Pd, and Pt, respectively.

As a further parameter the free activation energy ΔG^* can be extracted from the spectroscopic and electrochemical data acccording to the Hush–Marcus relation $\Delta G^* = (E_{IPCT})^2/4(E_{IPCT} - \Delta G_{12})$.[19] From these and the other data of Table 1 it is possible to draw the relative positions of the potential energy curves before and after electron transfer as given in Figure 7 for the system $MV[M(dmit)_2]$, M = Ni, Pd, and Pt, neglecting the weak splitting at the intersection point. A typical feature, as also evident from Table 1, is that the free energy of back-electron transfer ($\Delta G^* - \Delta G_{12}$) is always slightly larger for M = Ni and Pt (3–10 kJ/mol) than for M = Pd (2–6 kJ/mol). This corresponds to the stronger electronic coupling for the palladium complex, which should decrease the barrier between the minima of the two potential energy curves. For the $dmid^{2-}$ compounds **4b,4d** this activation energy is 11 and 14 kJ/mol, respectively.

Electrical Conductivity. Inspection of the trends in electrical conductivities (Table 1) suggests a separation of the compounds into two groups. For the nickel, palladium, and platinum complexes with the good acceptors **a**–**f** (class I) the conductivity increases with more negative ΔG_{12} values, while in the case of the poorer acceptors **g**–**i** and for all copper complexes (class II) a similar relation cannot be deduced with certainty. Polarization effects as proposed to occur in $(TTF)_2[M(mnt)_2]$, M = Pd and Pt,[4] may explain the fact that all platinum complexes have conductivities which in the average are about order of

(46) Curtis, J. C.; Meyer, T. J. *Inorg. Chem.* **1982**, *21*, 1562.

(47) Meyer, T. J. *Acc. Chem. Res.* **1978**, *11*, 94.
(48) Taube, H. *Ann. N.Y. Acad. Sci.* **1978**, *313*, pp 481, 496.

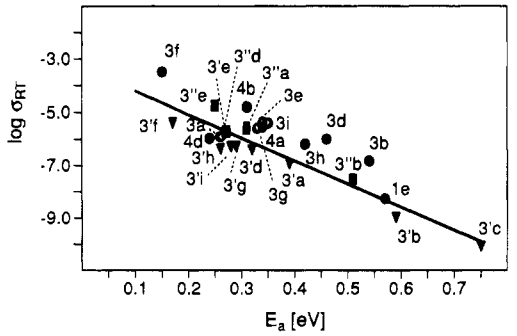

Figure 8. Plot of the logarithm of the specific electrical conductivity as function of the activation energy.

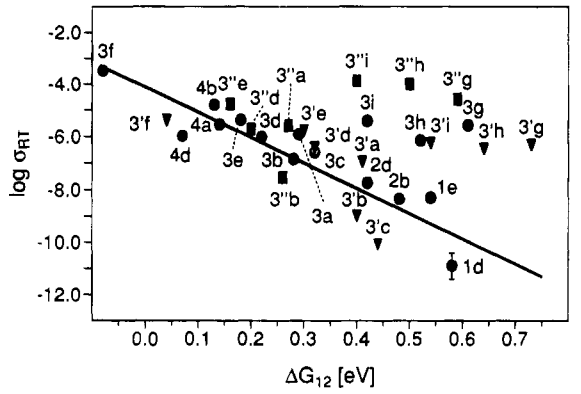

Figure 9. Plot of the logarithm of the specific electrical conductivity as function of ΔG_{12}.

magnitude larger than the corresponding nickel compounds although the ΔG_{12} values differ only by 0.02 eV (See Table 1).

A plot of log σ as function of the activation energy E_a for class I complexes reveals a linear relationship ($r = 0.87$, Figure 8) according to $\log \sigma = \log a - cE_a$, which indicates that variations of σ originate only in variations of E_a.[49] Since on the other hand the conductivity strongly depends on ΔG_{12}, it seems likely that log σ may change also with ΔG_{12} in a linear fashion. The corresponding plot (Figure 9) reveals that this is the case for class I compounds although the linear correlation is modest ($r = 0.88$) while it is much better ($r = 0.96$) when only the six compounds are considered which have the $[Ni(dmit)_2]^{2-}$ donor common. Keeping the latter constant may minimize the influence of steric factors on σ since the donor−acceptor arrangement should stay more constant than in the case the donor would be also varied.

Note that no similar relation, not even qualitatively, holds for the class II complexes. This applies for those d^8 complexes which posses strongly twisted acceptors as indicated e.g. by the almost constant log σ value of about −6.30 for the $[Pd(dmit)_2]^{2-}$ complexes of MQ^{2+}(**g**), BQ^{2+}(**h**), and PQ^{2+} (**i**) although ΔG_{12} changes from 0.73 to 0.64 and 0.54 eV, respectively (Table 1). In the case of the d^9 systems A[Cu(dmit)$_2$], which may have tetrahedral donor,[44] it even applies for approximately planar acceptors like DP^{2+} (**e**) and DPK^{2+} (**f**) as indicated by very similar values of log σ of −8.53 and −7.97 for **3*e** and **3*f**, respectively, although ΔG_{12} is 0.26 larger for the former ion pair.

From eqs 1 and 2 it follows that α^2, the amount of charge transferred from the donor to the acceptor, should increase with

(49) Ulbert, K. *J. Polymer. Sci. C.* **1969**, *27*, 881.

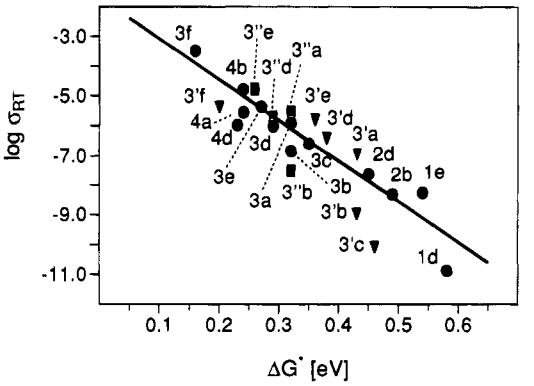

Figure 10. Plot of the logarithm of the specific electrical conductivity as function of the free activation enthalpy ΔG^* as calculated from the Hush−Marcus model.

decreasing ΔG_{12} values for a series of compounds having IPCT bands of similar integrated intensities and the same interionic distances. The results for class I complexes therefore suggests that the degree of charge transfer determines the conductivity. Since the presence of a nonplanar acceptor induces a different solid state structure as was demonstrated for the mnt^{2-} complexes BQ[Ni(dmit)$_2$],[35] it becomes plausible why class II compounds do not show the same dependence.

Since the amount of charge transferred should also increase with decreasing free activation energy of electron transfer, ΔG^*, one expects that log σ should increase with decreasing ΔG^*. As can be seen from Figure 10, the linear correlation is relatively poor ($r = 0.88$) when all complexes are taken into account (Figure 10, full line) while it is much better when only the six $[Ni(dmit)_2]^{2-}$ compounds are considered ($r = 0.96$). This means that charge generation occurs by electron transfer from the (dithiolene)metalate donor to the bipyridinium acceptor and that σ can be quantitatively predicted from the free activation energy of this process as calculated from redox potentials and the energy of the IPCT band.

Conclusion

The results presented above show that the Hush−Marcus model can be successfully applied to a large number of IPCT complexes by altering the driving force of electron transfer from 0.7 to about −0.1 eV. Reorganization energies and free activation energies (ΔG^*) of electron transfer calculated from this model are in the range of 0.83 and 0.2−0.7 eV. Although the electronic interaction between the two redox states is small, the specific electrical conductivity (σ) strongly depends on ΔG^* in the case of ion pairs with planar components (class I). No similar dependence is observed when one of the components is nonplanar (class II). For class I compounds σ increases by 8 orders of magnitude upon variation of ΔG^* and a plot of log σ as function of ΔG^* reveals an approximately linear dependence. This means that a solid state property can be quantitatively predicted from a parameter calculated from molecular electron-transfer theory.

Acknowledgment. Financial support by the Fonds der Chemischen Industrie and Volkswagen−Stiftung is gratefully acknowledged.

Supplementary Material Available: Two tables giving yields and analytical and IR data (2 pages). Ordering information is given on any current masthead page.